RSC Advances

ROYAL SOCIETY OF CHEMISTRY

www.rsc.org/advances

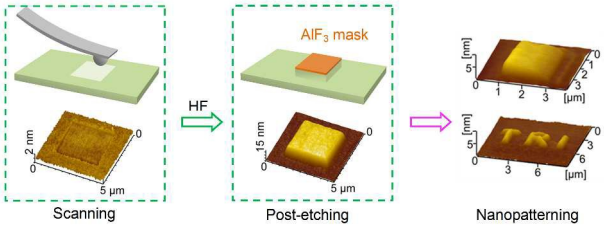

Graphical Abstract

A rapid and maskless method of nanofabrication on glass was proposed. The proposed method was based on the combined techniques of scanning with a diamond tip and post-etching in HF solution. The X-ray photoelectron spectroscopy confirmed that the masking effect should be attributed to the formation of insoluble AlF3 on the scan area during HF etching.

Journal Name

ARTICLE

Rapid and maskless nanopatterning of aluminosilicate glass surface via friction-induced selective etching in HF solution

Received 00th January 20xx,
Accepted 00th January 20xx

DOI: 10.1039/x0xx00000x

www.rsc.org/

Chenfei Song,[a,b] Bingjun Yu,[a] Mian Wang [a] and Linmao Qian*[a]

Protrusive nanostructures were fabricated with the proposed friction-induced selective etching method, which involves the combined techniques of scanning with an atomic force microscopy diamond probe and selective etching in HF solution. Various patterns, including slope and hierarchical stages, were produced by programming the loading mode and scanning traces. The height of such nanostructures increased as the scan load and number of scan cycles increased. X-ray photoelectron spectroscopy analysis indicated that the mechanism of the friction-induced selective etching should be attributed to the formation of AlF_3 on the fabrication area during HF etching. Given that the friction-induced selective etching could be completed in several seconds without any templates, the proposed method may provide high efficiency and serve as a convenient nanofabrication technique for glass.

Keyword: Friction, Selective etching, Glass, AFM, Nanofabrication

Introduction

Owing to its electrical isolation, high optical transparency, and chemical durability, glass has been widely used in micro/nanoelectromechanical systems, such as biochips, optical sensors, and storage devices [1–3]. One of the most popular nanofabrication methods for glass is photolithography, the application of which in a wide range of pattern sizes and mass production has achieved considerable success [4]. As the scaling down of device dimensions continues, lithographic technology has met technical challenges, including low flexibility, complicated processes, notching defects induced by masks, and so on [4]. In the effort to overcome such technical barriers, straightforward nanofabrication techniques have attracted much attention, and many maskless methods have been developed for nanofabrication on glass. For example, three-dimensional structures can be produced on glass surfaces via femtosecond laser direct writing, but the fabrication resolution needs to be improved further [5, 6]. Electron beam lithography is advantageous for nanofabrication because of its high resolution, but its high energy beam can cause the undesirable degradation of Si-O nets [7]. Even hollow structures can be created on glass surfaces after mechanical cutting, however, fracture damage and crack generation are serious problems that arise during the fabrication of such brittle materials [8–10]. These drawbacks have emphasized the importance of developing a novel method of nanofabrication on glass.

Recently, a friction-induced method based on atomic force microscopy (AFM) has been found to improve the possibility of performing nanofabrication without any templates or masks. Protrusive nanostructures can be directly fabricated via scanning with a diamond probe [11]. However, glass surfaces cannot endure repeated scanning, thereby limiting the height of hillocks to below 2 nm [11]. High nanostructures can be fabricated via friction-induced selective etching [12, 13]. Previous studies have suggested that mechanically densified layers in scan areas could act as a mask during HF etching, but the intrinsic causes of etching being restricted by the scanning process remain uncertain [14, 15]. To establish a reliable method of nanofabrication on glass, the friction-induced selective etching of glass must be studied further.

In the present study, protrusive nanostructures, such as slope and hierarchical stages, were fabricated by using a friction-induced selective etching method. The effect of scan load and number of scan cycles on the height of the nanostructures was also studied. The mechanism of the masking effect on the scan area was discussed on the basis of the comparison between the etching behaviors of amorphous SiO_2 and glass and the X-ray photoelectron spectroscopy (XPS) detection on a fabrication area. Given that the etching process could be finished in several seconds at room temperature, this friction-induced method will open new opportunities for nanofabrication of glass.

[a]*Tribology Research Institute, National Traction Power Laboratory, Southwest Jiaotong University, Chengdu 610031, Sichuan Province, P.R. China*
[b]*Key Laboratory of Material Tribology, Henan University of Science and Technology, Luoyang 471023, Henan Province, P.R. China*
[*]*Corresponding author: E-mail: linmao@swjtu.edu.cn, Tel.: +86 28 87600687, Fax: +86 28 87603142*

Materials and methods

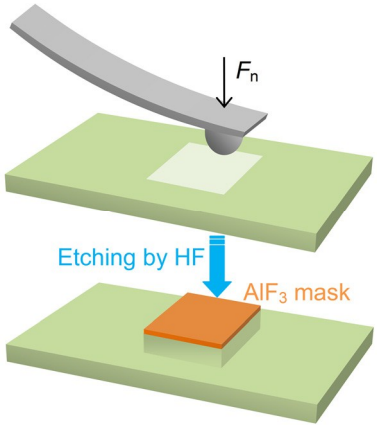

Figure 1 Sketch map of the fabrication process. Nanofabrication on glass can be achieved by scanning the target area and by selective etching in HF solution.

A harddisk glass with a thickness of 0.5 mm was purchased from Hoya Glass Disk Vietnam, Ltd. The root mean square roughness was measured with an atomic force microscope (SPI3800N, Seiko, Japan) at about 0.3 nm within an area in 1 μm × 1 μm. In addition to the trace elements found in the glass, such as Ca and K, the relative surface concentration ratio (atom.) of the main components of the glass was determined to be Al:Na:Si = 0.23:0.07:1. The fabrication process consisted of two steps: friction-induced scanning on the target area and selective etching in the HF solution (Fig. 1). During the scanning process, a diamond tip with an equivalent radius of 400 nm (Micro Star Technologies, USA) was used, and the spring constant of its cantilever was measured as 203 N/m by using a standard cantilever (CLFC-NOBO, Veeco, USA) [16, 17]. After scanning, the glass samples were etched in 20% HF solution at 293 K, unless otherwise specified. Our results showed that the formation of insoluble AlF_3 should result in the masking effect on the scan area. Protuberant nanostructures were then formed after HF etching. All the AFM images of the fabrication area were scanned with Si_3N_4 tips with a spring constant of 0.1 N/m (MLCT, Bruker Corp., USA).

To realize controllable nanofabrication, the effect of scan load F_n and number of scan cycles N on the height of the nanostructures h was investigated. During the scanning process, the scan load F_n varied from 5 μN to 33 μN, and the number of cycles N changed from 1 to 5. The scan area was set to 3 μm × 3 μm, and the scan speed was 12 μm/s. Finally, by programming the loading mode and scanning traces, demanded nanostructures could be fabricated at the target area on the glass surface. For example, a slope could be produced by scanning under progressive loads. With a fixed scan center, a hierarchical structure could be created by adjusting the scan size cycle by cycle. The nanoword "TRI" (which stands for Tribology Research Institute) could be written by scanning along the strokes of the letters.

To understand the fabrication mechanism, amorphous SiO_2 was etched in HF for comparison purposes. This material was chosen because its amorphous network is similar to that of glass. The amorphous SiO_2 consisted of pure silicon dioxide which was purchased from Semiconductor Wafer, Inc. (Hsinchu, Taiwan). Then, the chemical state of the fabrication area was detected by XPS using an Al $K\alpha$ X-ray source (ESCALAB 250, Thermo, USA). The XPS samples were produced via scanning with a homemade friction-induced nanofabrication equipment in an area measuring 300 μm × 300 μm under F_n = 2 mN, 10 mN, 15 mN. Given that the masking effect of the scan area could last for only several seconds at 293 K, the selective etching was performed at 273 K to extend the masking effect. The fabrication area could maintain its masking effect after etching for 30 s at 273 K. Therefore, the XPS samples were etched at 273 K for 15 s. Then, all of the spectra were calibrated against the C 1s peak of adventitious carbon at 284.5 eV.

Results

Friction-induced selective etching of aluminosilicate glass in HF solution

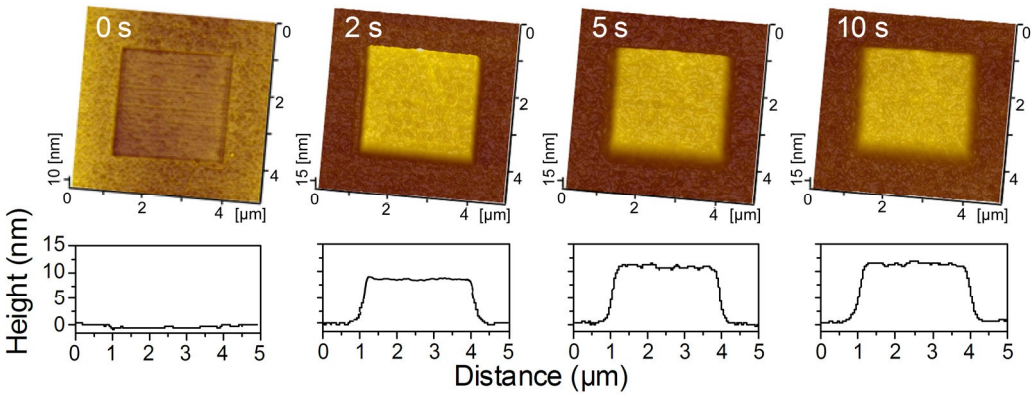

Figure 2 Effect of etching period on the height of the nanostructures. The number of scan cycles N was 1, and the scan load F_n was 33 μN. The sample was etched in 20% HF at 293 K.

Fig. 2 displays a typical friction-induced selective etching of a glass surface. The scanning was performed under a normal load of F_n = 33 μN for one cycle. After etching for 2 s in 20% HF at 293 K, a convex mesa with a height of 9.3 nm was formed on the scan area. When the etching period was increased to 5 s, the height of the nanostructure reached 11.1 nm. With the further increase of the etching period, the height of the pattern did not change a lot but the edge got blurring. To keep a sharp boundary, the etching period should not be longer than 10 s. We could develop a rapid and maskless method of nanofabrication on glass because the selective etching of glass could be completed in several seconds without any template or mask.

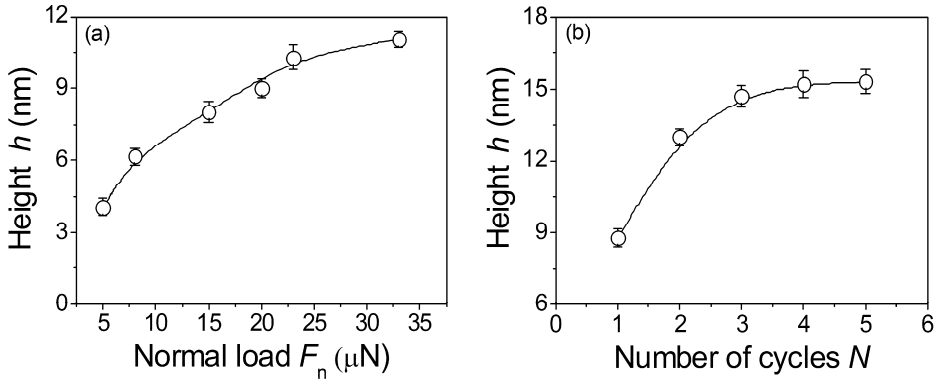

Figure 3 Effect of scan load F_n and number of scan cycles N on the height of the nanostructures h. (a) The scan load F_n ranged from 5 μN to 33 μN, and the number of scan cycles N was 1; (b) the number of scan cycles N increased from 1 to 5, and the scan load F_n was 20 μN. After scanning, the samples were etched in 20% HF at 293 K for 10 s.

Effect of scan parameters on the height of nanostructures

To realize controllable nanofabrication, we recognized the need to investigate the effect of scan parameters on fabrication height h. The scanning process was performed under various conditions of F_n = 5–33 μN and N = 1–5. After etching in 20% HF within adequate periods, the height of the scan area was plotted (Fig. 3). Both the scan load F_n and the number of scan cycles N showed significant effects on the fabrication height. As the scan load increased, the height of the nanostructures increased quickly and then reached 11.1 nm under F_n = 33 μN, as shown in Fig. 3a. In Fig. 3b, the height of the nanostructures increased rapidly and then slowly reached 15.3 nm under a constant scan load of 20 μN when the number of scan cycles increased from 1 to 5.

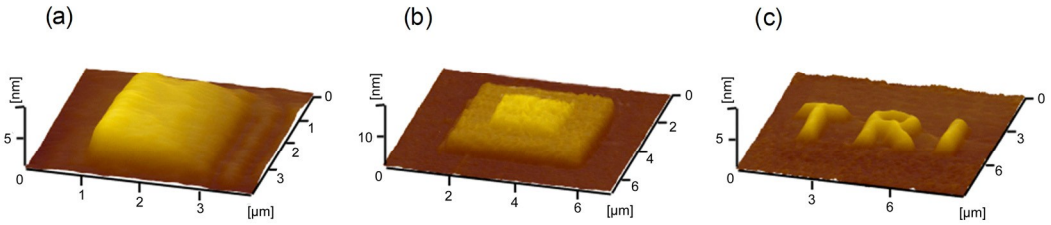

Figure 4 Rapid and maskless nanopatterning of a glass surface. (a) The slope was fabricated by scanning on a 2 × 3 μm^2 area under progressive loads ranging from 0 μN to 20 μN; (b) the hierarchical structure was fabricated by scanning under F_n = 20 μN, with the scan size of each cycle successively set to 4 and 2 μm; (c) the "TRI" pattern was written under 5 μN in one scan cycle. After scanning, the samples were etched in 20% HF for 10 s at 293 K.

Rapid and maskless nanopatterning of aluminosilicate glass surface

Various nanostructures can be produced by programming the loading mode and scanning traces. Fig. 4 shows the AFM images of typical nanostructures on glass produced by friction-induced selective etching. For example, the slope shown in Fig. 4a was formed after scanning on a 2 μm × 3 μm area under progressive loads ranging from 0 μN to 20 μN and etching for 10 s. The height of this nanostructure was 8.5 nm under the maximum load F_n = 20 μN. With a fixed scan center and F_n = 2[illegible] μN, the overlapped area was scanned in one more cycle when the scan size was set to 4 and 2 μm during repeated scanning. Therefore, a two-step hierarchical structure was formed after etching, with the steps reaching heights of 8.5 and 13 nm (Fig. 4b). The nanopattern of "TRI" in Fig. 4c was drawn by scanning along the strokes of the letters at F_n = 5 μN. After etching, the height of the letters was about 4 nm and the width was about

800 nm. To shrink the pattern dimension, smaller scan size should be designed and sharper tip should be selected. The minimal linewidth was about 250 nm under the given conditions.

Discussion

Effect of metal oxides on friction-induced selective etching

The networks of silica glass could be densified during scratching [18]. With XPS detection, Saito et al. observed that the structural changes of densified layers reduced the etching rated of glass in HF [15]. Iliescu et al. speculated that metal oxides could be formed into insoluble products such as AlF_3 during etching and even act as masking layers on glass surfaces [4, 19]. However, the formation of AlF_3 on fabrication area was not observed up to now. To clarify the mechanism of friction-induced selective etching, we compared the etching behavior in a scan area of pure SiO_2 and glass in HF solution. Before the etching, all the samples were scanned under 5 μN by one cycle.

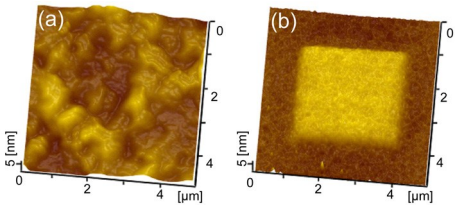

Figure 5 Comparison of etching behavior of amorphous SiO_2 (a) and glass (b) in HF solution. Before etching, all the samples were scanned by one cycle in a 3 × 3 μm^2 area under 5 μN.

As shown in Fig. 5a, no etching difference was observed in and outside the scan area on pure amorphous SiO_2. The etching reaction between the Si-O nets and the HF solution could be described as follows [4]:

$$SiO_2 + 4H^+ + 4F^- = SiF_4 \uparrow + 2H_2O \cdot \quad (1)$$

This reaction indicated that the pure Si-O nets could not resist the etching in the HF solution. However, a convex plate was formed on the scanned aluminosilicate glass surface after HF etching, as shown in Fig. 5b. The reactions of metal oxides in glass with HF could be described as [4, 20]

$$Al_2O_3 + 6H^+ + 6F^- = 2AlF_3 \downarrow + 3H_2O, \quad (2)$$

$$Na_2O + 2H^+ = 2Na^+ + H_2O \cdot \quad (3)$$

Insoluble AlF_3 may be generated during the HF etching of glass. Given that densification occurred on both the pure amorphous SiO_2 and the aluminosilicate glass [18], the comparison of their etching results suggested that metal oxides might perform an important function in the friction-induced selective etching of aluminosilicate glass.

Mechanism for the masking effect of the scan area

The lifetime of the mask layer in HF at room temperature was possibly too short (see Fig. 2). As a result, the masking effect of the fabrication area was difficult to maintain during the preparation of the XPS samples. To decrease the dissolution of the mask layer, selective etching was performed at 273 K. Given that the masking effect could last for about 30 s at 273 K, component evolution was detected by XPS after HF etching for 15 s at 273 K.

Take the sample scanned under 10 mN as an example, the measured spectrum shown in Fig. 6a indicated that about 51% of Al existed in the form of AlF_3 (76.1 eV) on the scan area [21, 22]. By contrast, most Al (83%) retained their oxide states (74.9 eV) on the original glass surface, as shown in Fig. 6b. For the Na 1s spectra, only one peak was observed at 1072.6 eV (Na-O) on both the scan area and the original area after etching, as shown in Figs. 6c and 6d [21]. These sharp contrasts between the chemical states of Al and Na suggested that the masking effect of the scan area was related to the formation of the insoluble AlF_3.

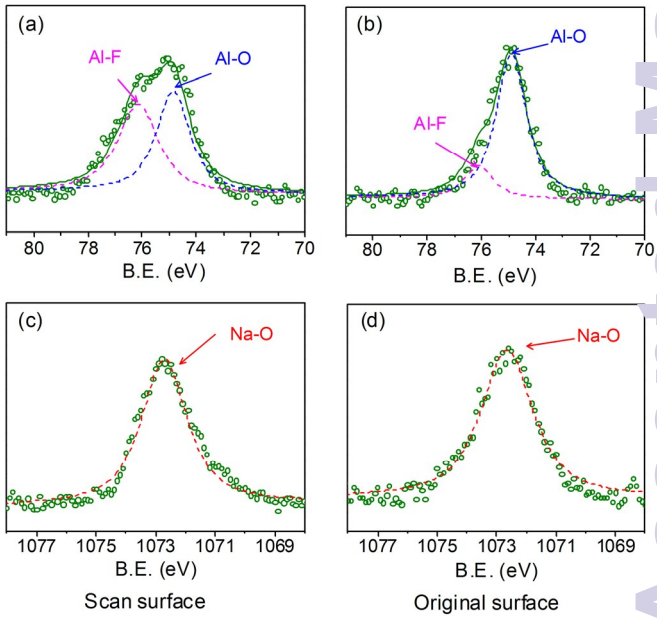

Figure 6 XPS Spectra of the surface scanned under 10 mN and original surface after etching at 273 K for 15 s. (a) and (b) Al 2p spectra; (c) and (d) Na 1s spectra. The sample was prepared by scanning under 10 mN. Spots: measured results. Solid lines: fitting lines. Dashed lines: multiple peak separation.

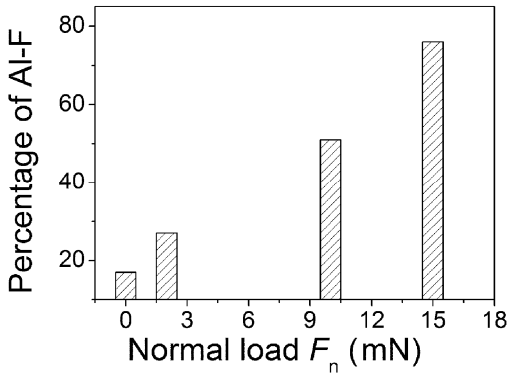

Figure 7 Effect of normal load on percentage of Al-F after etching in HF at 273 K for 15 s. The XPS samples were produced via scanning with a homemade friction-induced nanofabrication equipment in an area measuring 300 μm × 300 μm under F_n = 2 mN, 10 mN, 15 mN.

On the scanned area, a densified layer would form because the angle of Si-O-Si in glass decreased and the structures of glass was compressed during the scanning process[18]. Although the mass fraction of Al^{3+} ions did not change in the densified area, the compact degree of Al^{3+} ions in the glass networks increased due to the volume compression[23]. Therefore, the insoluble AlF_3 on the scan area should be denser than that on the original area during HF etching. Such AlF_3 could act as a mask layer to prevent leaching and the etching reactions of glass; protrusive nanostructures were then formed on the fabrication area [19, 24]. The rising of scan load was beneficial to the formation of AlF_3. As shown in Figure 7, with the scan load increased from 0 mN to 15 mN, the percent of Al-F increased from 17% to 73% on the XPS samples. Therefore the height of nanostructures increased with the increasing of normal load. NaF could not act as the etching mask because of its high solubility (see Figs. 6c and 6d). Although densification could also happen on amorphous SiO_2 and some sodalime glass (lower Al content) [15], no effective insoluble products could provide the masking effect, in which case friction-induced selective etching could not be carried out (see Fig. 5a). Finally, the results suggested that the formation of AlF_3 on the densified fabrication area should account for the friction-induced selective etching on the aluminosilicate glass.

In brief, nanofabrication on glass can be achieved via controllable scanning and post-etching in HF solution. The etching treatment can be finished in several seconds at room temperature, and this feature improves fabrication efficiency significantly. Various shapes of nanostructures can be obtained freely by programming scanning traces in the absence of any template. Compared with traditional lithography, the fabrication of hierarchical structures can be finished more easily during a single fabrication flow. As a force-assisted process, the friction-induced method is independent of electrochemical oxidation and is appropriate for nanofabrication on insulative glass. The results may help develop a rapid and maskless method of nanofabrication on glass. Mass production and linewidth reduction will be further researched for the application of the method.

Conclusions

In conclusion, a rapid and maskless method of nanofabrication on glass was developed on the basis of friction-induced selective etching. Various protrusive nanostructures, including slope and hierarchical stages, were produced by scanning with a diamond tip and fast etching in HF solution. The height of such structures increased to 15.3 nm as the scan load or/and number of scan cycles increased. The XPS results showed that the etching mask effect could be attributed to the formation of AlF_3 on the densified fabrication area. Given that the etching process could be finished in several seconds at room temperature without any templates, the proposed method can open up new opportunities for nanofabrication on aluminosilicate glass.

Acknowledgments

The authors are grateful for the financial support from National Natural Science Foundation of China (91323302, 51305365, 51375409).

References

1 C. R. Vistas, A. C. P. Águas and G. N. M. Ferreira, *Appl. Surf. Sci.* , 2013, **286**, 314-318.
2 H. Zhang, S. M. Eaton, J. Li, A. H. Nejadmalayeri and P. R. Herman, *Opt. Express*, 2007, **15**, 4182-4191.
3 K. Dae Hong, K. Yong Kwan, H. Seungbum, K. Yunseok and B. Sunggi, *Nanotechnology*, 2011, **22**, 245705.
4 C. Iliescu, B. Chen and J. Miao, *Sens. Actuators A*, 2008, **143**, 154-161.
5 L. Li, M. Hong, M. Schmidt, M. Zhong, A. Malshe and V. Kovalenko, *Cirp Ann-Manuf. Techn.*, 2011, **60**, 735-755.
6 Y. Liao, Y. Shen, L. Qiao, D. Chen, Y. Cheng, K. Sugioka and K. Midorikawa, *Opt. Lett.*, 2013, **38**, 187-189.
7 K. Zheng, C. Wang, Y. Q. Cheng, Y. Yue, X. Han, Z. Zhang, Z. Shan, S. X. Mao, M. Ye, Y. Yin and E. Ma, *Nat. Commun.*, 2010, **1**, 24.
8 Y. Yan, T. Sun, X. Zhao, Z. Hu and S. Dong, J. *Micromech. Microeng.*, 2008, **18**, 035002.
9 B. Tanikella and R. Scattergood, *Scripta Mater.*, 1996, **34**, 207-213.
10 J. Yu, Q. Jian, W. Yuan, B. Gu, F. Ji and W. Huang, *Appl. Surf. Sci.*, 2014, **292**, 267-277.
11 B. Yu, H. Dong, L. Qian, Y. Chen, J. Yu and Z. Zhou, *Nanotechnology*, 2009, **20**, 465303.
12 Y. Saito, S. Okamoto, A. Miki, H. Inomata, T. Hidaka and H. Kasai, *Appl. Surf. Sci.*, 2008, **254**, 7243-7249.
13 S. Youn and C. Kang, *Scripta Materialia*, 2005, **52**, 117-122.
14 Y. Saito, S. Okamoto, H. Inomata, J. Kurachi, T. Hidaka and H. Kasai, *Thin Solid Films*, 2009, **517**, 2900-2904.
15 Y. Saito, S. Okamoto, H. Inomata and J. Kurachi, *Appl. Surf. Sci.* , 2008, **255**, 2290-2294.
16 A. Torii, M. Sasaki, K. Hane and S. Okuma, *Meas. Sci. Technol.*, 1996, **7**, 179-184.
17 M. Wang, S. Cui, B. Yu and L. Qian, Sci. *China Technol. Sci.*, 2013, **56**, 2927-2933.
18 Y.-F. Niu, K. Han and J.-P. Guin, *Langmuir*, 2012, **28**, 10733-10740.
19 C. Iliescu, J. Jing, F. E. H. Tay, J. Miao and T. *Sun, Surf. Coat. Technol.*, 2005, **198**, 314-318.
20 G. A. C. M. Spierings, *J Mater Sci*, 1993, **28**, 6261-6273.
21 L. Lallement, C. Gosse, C. Cardinaud, M.-C. Peignon-Fernandez and A. Rhallabi, *J. Vac. Sci. Technol. A*, 2010, **28**, 277-286.
22 P. J. Matsuo, T. E. F. M. Standaert, S. D. Allen, G. S. Oehrlein and T. J. Dalton, *J. Vac. Sci. Technol. B*, 1999, **17**, 1435-1447.
23 T. Taniguchi, *Physics and Chemistry of Glasses*, 2004, **45**, 183-191.
24 C. Iliescu, F. E. Tay and J. Miao, *Sens. Actuators A*, 2007, **133**, 395-400.